Determination of the anticorrosive properties oftrimebutinemaleateforaluminum corrosion in 2M HCl. Gravimetric and quantum chemistryapproaches.

ABSTRACT

The present work evaluated the inhibition properties of (R,S)-2-(dimethylamino)-2-phenylbutyl 3,4,5-trimethoxybenzoate or trimebutine maleate in aluminum corrosion in 2M hydrochloric acid. Tests were carried out using gravimetric methods and density functional theory (DFT). The results indicate that trimebutine maleate is a good inhibitor of aluminum corrosion in 2M hydrochloric acid at low temperatures. Indeed, the inhibition efficiency of this molecule increases with increasing concentration and decreases with increasing temperature. For an inhibitor concentration of 5.2mM and at 298K, we obtained an inhibition efficiency of 93.61%. The adsorption process is spontaneous, exothermic and follows the Langmuir model. The activation parameters were calculated and analyzed. Density functional theory at the B3LYP/6-311G(d.p) level was used to determine molecular parameters such as EHOMO, ELUMO, ΔE, η, S, μ , A, I, χ, ΔN, ω. These parameters were used to explain the inhibition efficiencies obtained. Local selectivity was analyzed using Fukui functions and the dual descriptor to determine possible nucleophilic and electrophilic attack sites.

Keywords: Trimebutine maleate; Corrosion; aluminum, Hydrochloric acid, Density functional theory, gravimetric methods.

1. INTRODUCTION

The search for corrosion inhibitors capable of reducingmetal corrosion has become a major preoccupation for researchers in thisfield[1]. Corrosion causes enormousmaterial damage, which continues to have a negative impact on the economies of manyindustrialsectors[2].
However, corrosion can becontrolled by numerousmethods, including corrosion inhibitors. In thiscontext, severalorganic compounds have been used to preventaluminum corrosion in hydrochloricacid solutions [3,4,5,6].
Aluminium and itsalloys due to theirlowcost, light weight, lowdensity, good appearance and high thermal and electricalconductivity are widelyused in many businesses [7]. In use, aluminum and itsalloysbecomecoatedwith corrosion products. Hydrochloricacid, for example, isused to maintainaluminumequipment[8].
Research has been carried out to findinexpensive, non-toxic, natural and eco-friendly inhibitors for the protection of metals and alloysagainst corrosion in acid solutions duringthis maintenance [9,10,11].Someorganic and inorganic corrosion inhibitors effective in combatingmetaldegradation in saidacid solutions are toxic[12]. Their use poses problems for the environment and humanhealth. In recentstudies, researchers have turned to green

sources or plant extracts and drugs[13,14,15].These efforts directedtowardsthese compounds are justified by theiraccessibility and non-toxicity. Compounds containingheteroatoms or heterocycles have the ability to slow down the dissolution of aluminum in acid solutions and replace toxicinhibitors.

These compounds or molecules, by virtue of their structure containingatoms (O, N and S), are likely to bind to the aluminum surface to form an adsorption layer. This type of layer reduces the loss of electronsfrom the metal in the aggressive solution. Based on this information, drugssuch as antivirals[16], antihypertensives [17],antihistamines[18], antidiabetics[19] and vitamins[20] have been used to inhibitmetal corrosion. Therefore, thisstudyconsists in testing the inhibition properties of (R,S)-2-(dimethylamino)-2-phenylbutyl 3,4,5-trimethoxybenzoate or trimebutinemaleate in aluminum corrosion in 2M HCl. This compound is an antispasmodic, as itisused in the symptomatictreatment of spasmodic intestinal pain. It helpsrelieve transit disorders and intestinal discomfortassociatedwithfunctionalbowelproblems.

In thisstudy, densityfunctionaltheory, a theoreticalmethod, wasused to accompany the experimentalmethod. This combination will help explain the inhibition mechanism as well as the electronic exchanges between the molecule and the metal. Specifically, inhibitoryefficiencies, adsorption type, adsorption and activation thermodynamicquantities, and local and global reactivity quantum descriptorparameterswereredetermined.

2. MATERIAL AND METHODS

2.1 Solution test preparation

All reagents and solventsused in the experimentwere of analytical grade and usedwithoutfurther purification. The aggressive solution of 2.0 M HClwasprepared by diluting the analytical grade 37% (Merck Chemicals) withdistilled water. Acetonefrom Sigma Aldrich withpurity: 99.5%. The inhibitortrimebutinemaleate(figure1) wasacquiredfromSinopharmchemicalreagent. Four concentrations have been preparedfromthisinhibitorwhich are 0.26mM; 0.52mM; 1.3mM; 5.2mM.

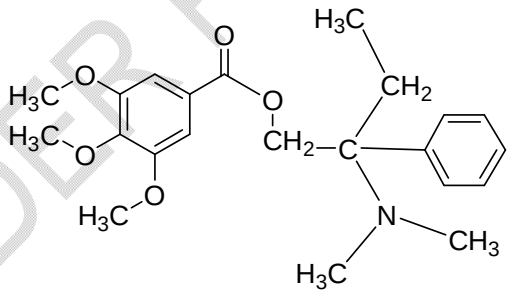

Fig 1 : Chemical structure of trimebutine maleate (TM)

2.2. Aluminumsamplespreparation

The aluminumsampleswere in the form of rodmeasuring 10mm in length and 2mm in diameter. The sampleswerepolishedwith abrasive paperrangingfrom 150 to 600 grit, cleanedwithacetone, washedwithdistilled water and dried in an oven. The sampleswerethenweighed (m_1).

2.3.Weightlossmeasurements

Eachsampleisimmersedin 50 mL HCl-2M with or without the various concentrations of trimebutinemaleate.After 1h immersion, the sampleisremovedfrom the solution and rinsedthoroughlywithdistilled water. It isdried, thenreweighed (m_2). Each test wasrepeatedat 298 K, 308 K, 318 K, 328 K and 338 K.
Weightlossmeasurements($\Delta m = m_1 - m_2$) wereused to deduce the average corrosion rate of aluminum (W), the rate of surface coverage(θ) and the inhibitor inhibition efficiencyIE(%) as a function of set temperature and inhibitor concentration. Theseparameterswereobtainedfrom the followingequations:

- $W = \frac{\Delta m}{S_e.t} = \frac{m_1 - m_2}{S_e.t}$(1)
- $\theta = \frac{W_0 - W}{W_0}$ (2)
- $IE(\%) = \frac{W_0 - W}{W_0} * 100$(3)

2.4.Thermodynamic adsorption and activation determinationmethod

The possibility of the adsorption reactionisindicated by the variation in standard free enthalpy of adsorption ΔG^0_{ads}. This quantity is determined from the relationship below [21].

- $\Delta G^0_{ads} = RTln\,(55.5\,K_{ads})$ (4)

Where : K_{ads}isthe adsorption constant, 55.5isthe concentration of water (in mol/L) in the solution; R is the perfectgas constant; Tisabsolutetemperature.
Quantitiessuch as adsorption enthalpy (ΔH^0_{ads}) and adsorption entropy (ΔS^0_{ads}) are deduced from the Gibbs relation:

- $\Delta G^0_{ads} = \Delta H^0_{ads} - T\Delta S^0_{ads}$ (5)

Activation parameterssuch as activation energy (E_a), enthalpyactivation (ΔH^*_a) and entropy activation (ΔS^*_a) are calculatedfrom the following expressions

- $W = Aexp\left(-\frac{E_a}{RT}\right)$(6)
- $W = \frac{R.T}{N_A.h} exp\left(\frac{\Delta S^*_a}{R}\right).exp\left(-\frac{\Delta H^*_a}{R.T}\right)$(7)
- $log\left(\frac{W}{T}\right) = log\left(\frac{R}{N_A.h}\right) + \frac{\Delta S^0_a}{2,3.R} - \frac{\Delta H^0_a}{2,3.R.T}$(8

Where$E_a$is the activation energy, R is the perfectgas constant, T is the absolutetemperature and A is the frequency factor. $N_A$is Avogadro's number.

2.5.Theoreticalapproach: quantum chemicalcalculations

Density Functional Theory (DFT) based on quantum chemicalcalculationswasused to explain the experimental data. Experimentalresults can beused to determine the inhibition efficiencyof the moleculestudied.While DFT can beused to explain the mechanism by which

the moleculeprotects the metal. All calculationswereperformedwithGaussian 09 software using 6-311G (d, p) basis set [22] withBecke'sthree-parameterhybrid (B3LYP) [23].Geometricoptimizationwascarried out under the same conditions, and the relevant parameterswerecalculated. Theseparameters are highest occupied molecular orbital energy (E_{HOMO}), lowest unoccupied molecular orbital energy (E_{LUMO}),dipole moment (μ) and total energy (E_T).Using the mathematical relationships expressed below, other parameters such as energy gap (ΔE), ionization energy (*I*), electron affinity (*A*), electronegativity(χ), , softness (σ), hardness (η) and electrophylicity index (ω), fraction of electrons transferred (ΔN) have been determined [24,25,26,27,28,29,30].

- $\Delta E = E_{\text{LUMO}} - E_{HO\text{MO}}$ (9)
- $I = -E_{\text{HOMO}}$ (10)
- $A = -E_{\text{LUMO}}$ (11)
- $\chi = \frac{I+A}{2} = -\frac{E_{LUMO}+E_{HOMO}}{2}$ (12)
- $\sigma = \frac{1}{\eta} = \frac{2}{I-A}$(13)
- $\eta = \frac{I-A}{2} = \frac{E_{LUMO}-E_{HOMO}}{2}$ (14)
- $\omega = \frac{\mu_P^2}{2\eta} = \frac{(I+A)^2}{4(I-A)}$ (15)
- $\Delta N = \frac{\phi_{Al}-\chi_i}{2(\eta_{Al}+\eta_i)}$(16)

Whereχ_{inh}andϕ_{Al} represent electronegativities of the inhibiting molecule and the metal respectively while η_{inh} and η_{Al}represent the hardness of the inhibiting molecule and metal respectively. The theoretical value of Al (ϕ_{Al} = 4,28 $eV, and \eta_{Al}$ = 0)wereused to calculate the number of transferredelectrons.

3. RESULTS AND DISCUSSION

3.1. Temperature and inhibitor concentration action on aluminum corrosion rate

Figure2 shows the evolution of corrosion rate as a function of TM concentration and reaction medium temperature.

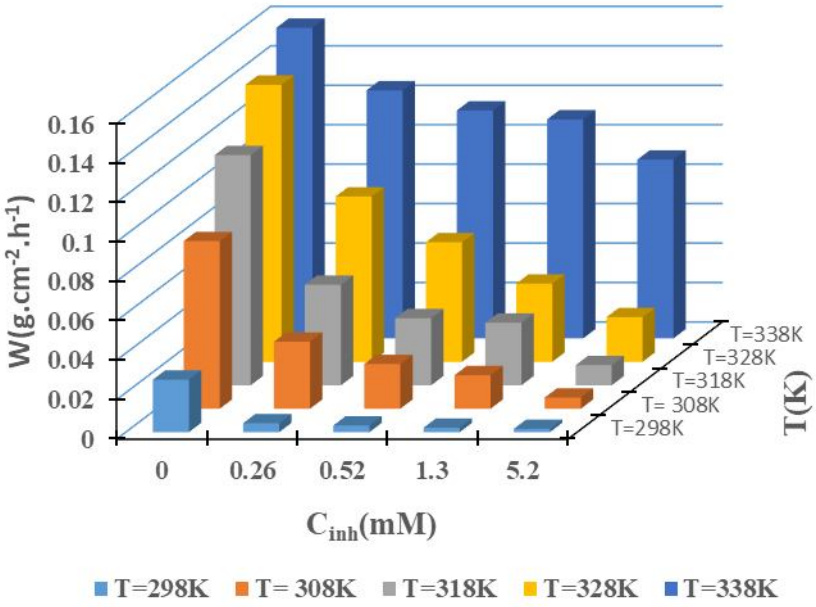

Fig. 2. Corrosion rate versus temperature and TMconcentration

Figure 2 shows that the corrosion rate decreasesprogressivelywithincreasing MT concentration. It alsoappearsincreasingtemperature leads to a rapid change in the corrosion rate of aluminum. This rate increasessharply in the absence of inhibitor. Theseresultsclearlyindicatethat the addition of TM to the corrosive solution slows down aluminum dissolution. Hydrogen ions in solution promotealuminumoxidation. This oxidation, whichincreaseswithtemperature, isreduced by the presence of trimebutine.

3.2. Influence of temperature and inhibitor concentration on inhibition efficiency

The progression of inhibitionefficiency as a function of TM concentration and reaction medium temperatureisillustratedby Figure 3.

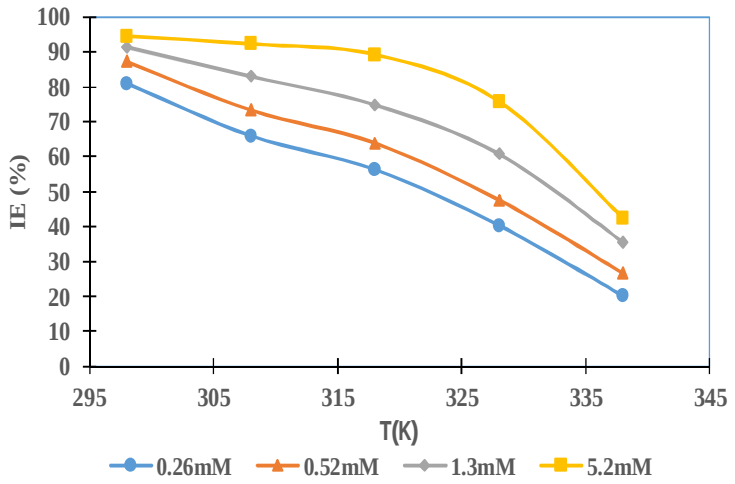

Fig.3. Evolution of Inhibition Efficiency as a Function of Temperature

Examination of Figure 3 shows that the inhibition efficiency decreases as the temperature of the corrosive solution rises, and increases as the concentration of TM increases. These results show that the molecule adsorbs weakly to the aluminum surface as the temperature rises. In fact, the dissolution of aluminum in 1M HCl solution increases as temperature rises. Thus, when this loss of electrons becomes significant, the electrons supplied by trimebutine maleate are not sufficient to replace them, which explains why the efficiency of inhibition decreases with increasing temperature. The increase in inhibition efficiency with increasing concentration is due to the adsorption of trimebutine maleate on the aluminum surface. In addition, the adsorbed layer on the metal surface becomes increasingly compact as the inhibitor concentration increases. This adsorption is aided by the presence of oxygen and nitrogen atoms, electron pairs and π-electrons on the molecule's aromatic nuclei. The metal surface is thus covered with a protective layer that reduces the effects of oxidizing ions.

3.3. Adsorption isotherm studies

The study of the adsorption mode provides information on the characteristics of the MT adsorption process on the aluminum surface. The models of Langmuir, Temkin, El-Awady and Freundlich were tested in order to identify the one that correctly describes the behavior of TM on the metal surface. This study is based on the relationship between recovery rate (θ) and inhibitor concentration (Cinh). To determine the nature of adsorption, the Adejo-Ekwenchi model was used. The equations for these isotherms are given by the following relationships **[31,32, 33,34,35]:**

- Isotherme de Langmuir : $\frac{\theta}{1-\theta} = K_{ads}.C_{inh}$(16)
- Isotherme de Temkin : $\theta = \frac{2,303}{f}[logK_{ads} + logC_{inh}]$(17)
- El-Awady : $log\left(\frac{\theta}{1-\theta}\right) = \log K_{ads} + ylogC_{inh}$(18)
- Freundlich: $\theta = K_{ads}.C_{inh}^{1/n}$ (19)
- Adejo- Ekwenchi :$log\left(\frac{1}{1-\theta}\right) = logK_{AE} + blogC_{inh}$(20)

Where, f: coefficient related to lateral interactions between molecules in the adsorption layer, K_{ads}: adsorption equilibrium constant, $1 / y = x$ expresses the number of active sites occupied by an inhibitor molecule; b is the parameter of the Adejo Ekwenchi isotherm and K_{AE}: adsorption equilibrium constant of the Adejo Ekwenchi model.

Figures4, 5, 6 and 7 illustrate the representations of the different isotherms. The parameters of the isotherms studied are given in Table 1.

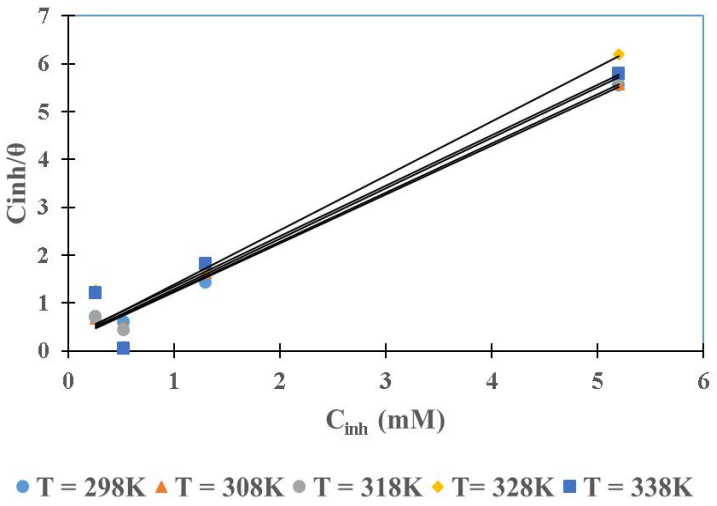

Fig. 4.Langmuir adsorption isotherm plots of TM on aluminium in 2M HCl

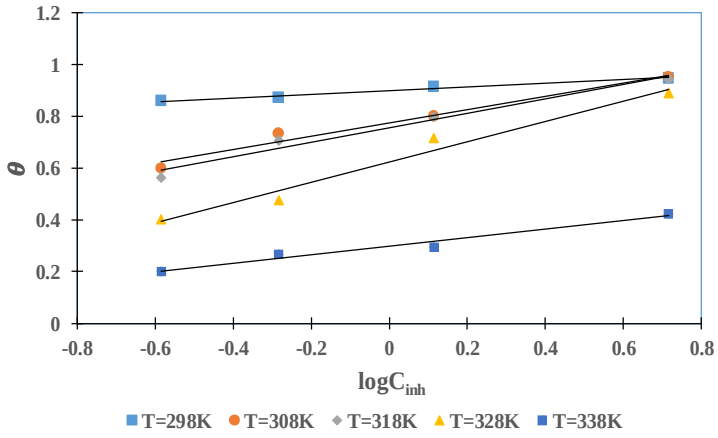

Fig. 5.Langmuir adsorption isotherm plots of TM on aluminium in 2M HCl

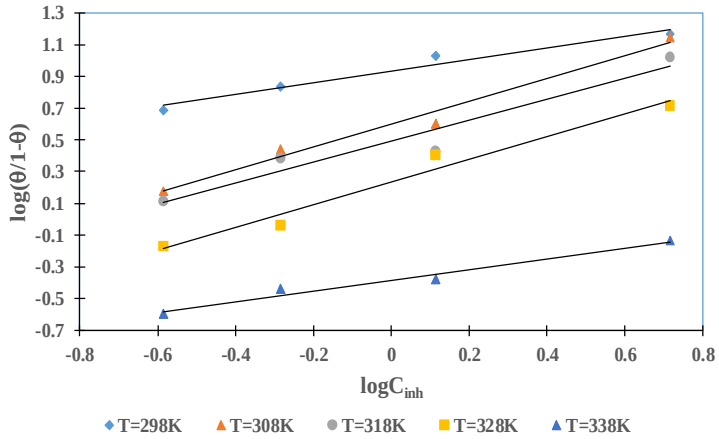

Fig.6.EL-Awady adsorption isotherm plots of TM on aluminium in 2M HCl

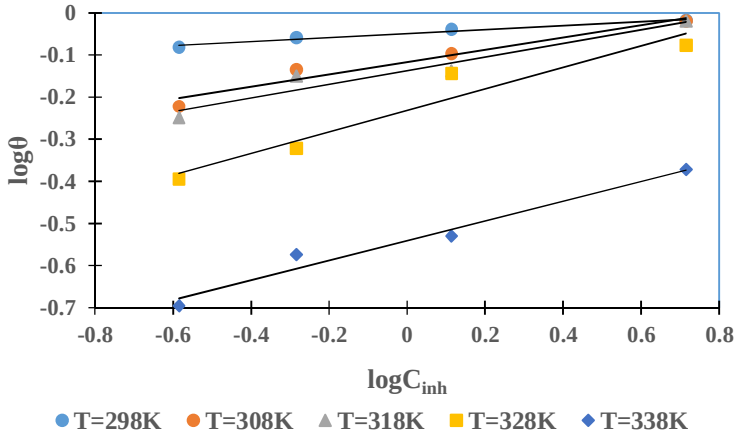

Fig.7. Freundlich adsorption isotherm plots of trimebutine on aluminium in 2M HCl

Table 1. Isotherms parameters for various temperatures

Isotherms	T(K)	Slope	Intercept	(R^2)
	298	1.0208	0.2133	0.9944
	308	1.0291	0.2208	0.9942
Langmuir	318	1.0541	0.2357	0.9958
	328	1.0417	0.2464	0.9934
	338	1.0542	0.2968	0.9955
	298	0.0697	0.899	0.9745
	308	0.2580	0.7742	0.9747
Temkin	318	0.2790	0.7559	0.9713
	328	0.3917	0.6252	0.9720
	338	0.1642	0.2984	0.9707
	298	0.3685	0.9337	0.9625
	308	0.722	0.5980	0.9816
El-Awady	318	0.6572	0.4922	0.9338

	328	0.7164	0.2342	0.9711
	338	0.3397	0.3840	0.9732
	298	0.0470	-0.0489	0.9695
	308	0.1456	-0.1169	0.9522
Freundlich	318	0.1615	-0.1375	0.9320
	328	0.2553	-0.2319	0.9293
	338	0.2344	-0.5410	0.9694

Analysis of the parameters of the lines for the various isotherms indicates that the coefficients of determination (R^2) for the Langmuir model are closer to unity than those for the other models. In addition, the slopes of the Langmuir isotherm lines are approximately equal to one. Consequently, the adsorption of TM follows Langmuir adsorption model. During adsorption of the inhibitor on aluminium surface, each site can adsorb only one particle and the adsorption energy is constant. Furthermore, interactions between adsorbed particles are negligible [30].

The Adejo-Ekwenchi isotherm has been used to specify the nature of adsorption, i.e. the temperature ranges where chemisorption and physisorption take place [35]. The representation of this isotherm is given in Figure 8. The parameters of this isotherm are given in Table 2.

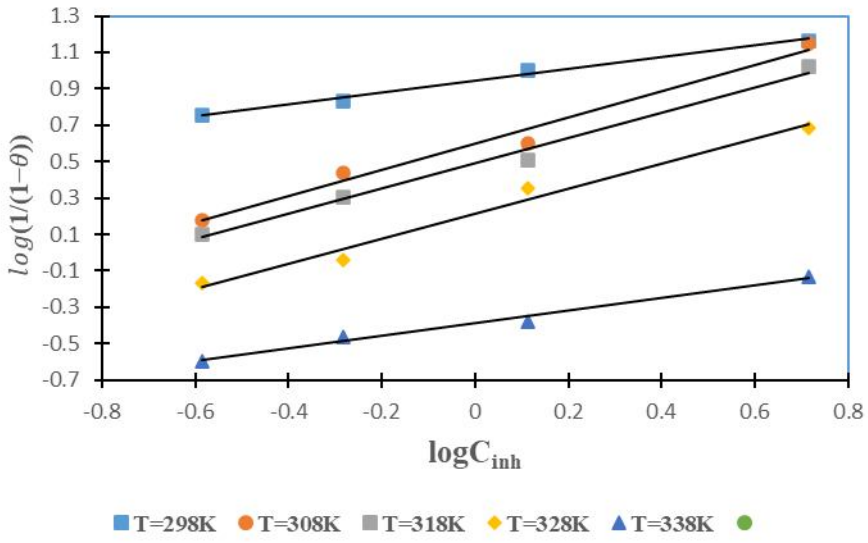

Fig.8. Adejo-Ekwenchi isotherm plots of trimebutine on aluminium in 2M HCl variation of $log\left(\frac{1}{1-\theta}\right)$as a function of $logC_{inh}$

Table 2. Values of thermodynamic adsorption quantities.

T(K)	Equations	R^2
298	$log\left(\frac{1}{1-\theta}\right)$ = 0.3222$logC_{inh}$ + 0.9432	0.9917
308	$log\left(\frac{1}{1-\theta}\right)$ = 0.722$logC_{inh}$ + 0.598	0.9816
318	$log\left(\frac{1}{1-\theta}\right)$ = 0.6968$logC_{inh}$ + 0.4901	0.9888
328	$log\left(\frac{1}{1-\theta}\right)$ = 0.6859$logC_{inh}$ + 0.2136	0.9814
338	$log\left(\frac{1}{1-\theta}\right)$ = 0.3455$logC_{inh}$ + 0.3889	0.9854

The slopes of the straight lines obtained, which represent the parameter b of this isotherm, increase from 298K to 308K.This increase indicates that trimebutine maleate adsorbs to the metal by covalent bonds (chemical adsorption). On the other hand, the values of b decrease from 308K to 338K. In this case the molecule adsorbs to the aluminium surface by electrostatic interactions (physical adsorption). It can be deduced from this that the adsorption of the inhibitor on the aluminium surface is dominated by physisorption. This type of adsorption does not promote effective protection of the metal against corrosion at high temperatures [36].

3.4. Thermodynamic study of the inhibition process

3.4.1.Thermodynamic quantities of adsorption

The changes in standard adsorption-free enthalpy values obtained from expression (3). These values were used to deduce the standard adsorption enthalpy (ΔH^0_{ads}) and entropy(ΔS^0_{ads}) change using Figure9. The values of these quantities are listed in Table 3.

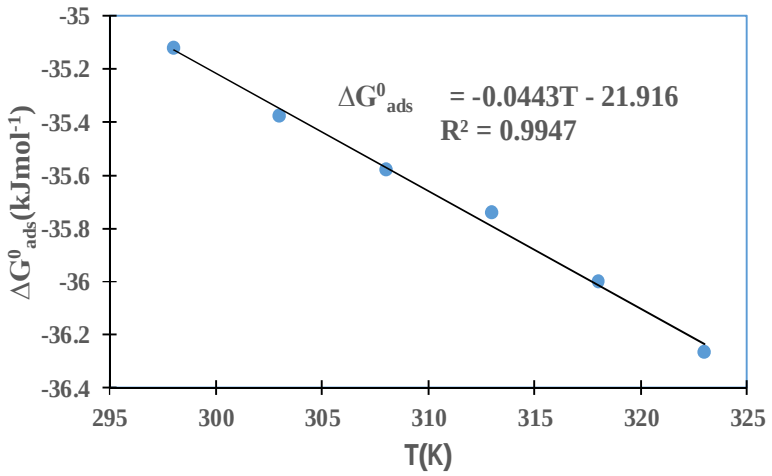

Fig. 9. Evolution of ΔG^0_{ads} as a function of temperature

Table 3. Values of thermodynamic adsorption quantities

T(K)	K_{ads}	ΔG^0_{ads} $(kJ.mol^{-1})$	ΔH^0_{ads} $(kJ.mol^{-1})$	ΔS^0_{ads} $(J.mol^{-1}K^{-1})$
298	4688.232536	-30.91562072		
308	4531.037608	-31.82736227		
318	4255.319149	-32.69481385	-21.916	44.300
328	4058.441558	-33.59383523		
338	3369.272237	-34.09531716		

The values of K_{ads} decrease progressively as the temperature increases. This decrease relates to the desorption of inhibitor molecules from the aluminum surface [31]. These molecules become increasingly detached from the aluminum surface as the temperature rises. These data explain the decrease in TM inhibition efficiency as the temperature rises. In this case, the increase in temperature is unfavourable to the adsorption of TMon metal surface in hydrochloric acid solution.

The values of $\Delta G^0_{ads}$are negative, so the inhibitor adsorption process is spontaneous and the adsorbed layer is stable. In addition, the values of $\Delta G^0_{ads}$are between -20 kJ.mol^{-1} and -40 kJ.mol^{-1}. In this case, the adsorption process is both chemical and physical [37,38]. The exothermicity of the adsorption process is indicated by negative values of ΔH^0_{ads}[39]. The positive values of ΔS^0_{ads}mention that this process is accompanied by an increase in disorder [39]. This disorder is due to the detachment of water molecules from the metal surface.

3.4.2.Thermodynamic activation factors

Representations of $logW$ as a function of $1/T$ (Figure 10) and log (W/T) as a function of $1/T$ (Figure 11) for different inhibitor concentrations allow the activation energy $(\boldsymbol{E_a})$, activation enthalpy $(\Delta H^*_a)$and activation entropy$(\Delta S^*_a)$to be calculated.

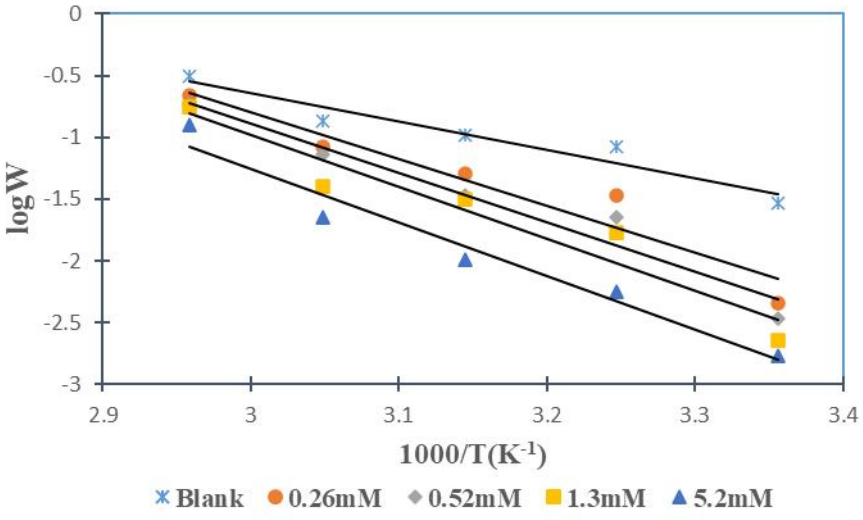

Fig. 10.Variation of logW**as function of** 1/T

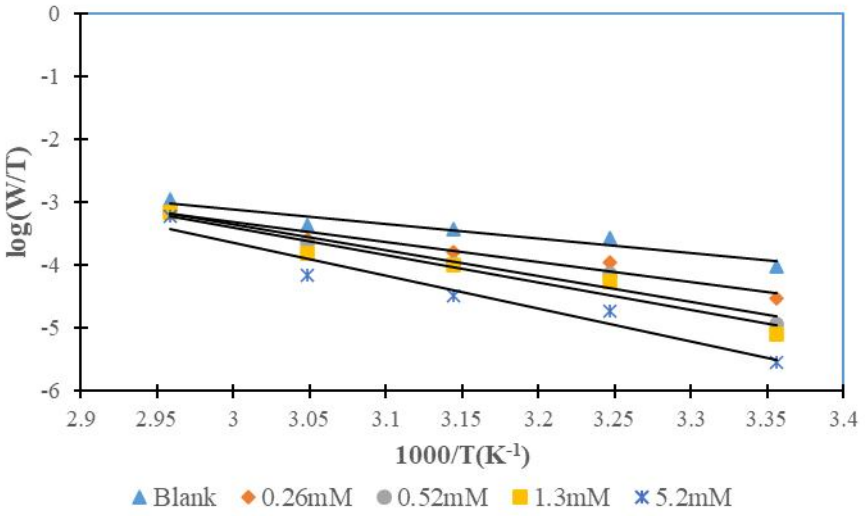

Fig. 11.Variation of $logW/T$ as function of $1/T$

Table 4. Thermodynamics Activation Parameters

C_{inh} (mM)	$E_a(kJ.mol^{-1})$	$\Delta H_a^*(kJ.mol^{-1})$	$\Delta H_a^*(kJ.mol^{-1})$
0	43.93991347	44.5511481	-123.5955968
0.26	73.03583123	60.70000518	-79.165632
0.26	77.09220646	78.19012947	-27.4525056
1.3	80.40705254	83.81578733	-11.5370944
5.2	83.31185408	100.0911068	32.646016

Analysis of Table 4 shows that activation energy values in the inhibited solutions are higher than those in the control. These data show that aluminium dissolution is rapid in the absence of TM and slow in its presence. This dissolution becomes slower and slower as the concentration of the inhibitor increases. The enthalpy of activation values are positive and increase with inhibitor concentration. These values show that aluminum dissolution in HCl-2M is endothermic and is reduced in the presence of the inhibitor [40]. Moreover, the activation entropy values indicate that this reduction is accompanied by a decrease in disorder. Similar results have been obtained in previous studies [41].

3.5. Theoretical analysis of the inhibition mechanism

3.5.1 Analysis of global reactivity parameters

The optimised structure of the molecule studied by DFT in B3LYP/6-311G(d,p) is given in Figure12. The global reactivity parameters are listed in Table 5.

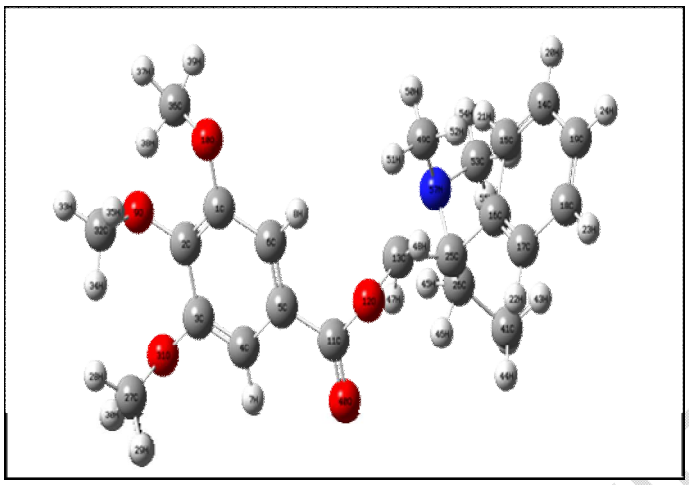

Fig. 12. Optimised structure of trimebutine maleate

Table 5. Global reactivity parameters of trimebutine maleat by B3LYP/6-31G(d, p)

Parameters	6-311G(d, p)
E_{HOMO} (eV)	-5.7952
E_{LUMO} (eV)	-2.5941
Energy gap ΔE (eV)	3.2011
Dipole moment μ (D)	5.2427
Ionization energy I (eV)	5.7952
Electron affinity A (eV)	2.5941
Electronegativity χ (eV)	4.1947
Hardness η (eV)	1.6006
Softness (σ) (eV)-1	0.6248
Fraction of electron transferred ΔN	0.0266
Electrophylicity index ω	5.4967
Energie totale E_T (Ha)	-1286.2922

Molecular reactivity descriptors for TM have been calculated to explain the experimental values obtained. Indeed, the highest occupied molecular orbital energy (E_{HOMO}) obtained is high. Consequently, the molecule has the capacity to donate electrons to aluminum [42]. The lowest unoccupied molecular orbital energy (E_{LUMO}) obtained indicates that the molecule can receive electrons from the metal [42]. It has been reported that the adsorption of an inhibitor to a metal surface is often linked to its electron donor-acceptor relationship with the metal. The results indicate that the molecule studied can both donate and receive electrons from aluminum. These properties justify the high inhibitory efficiencies obtained experimentally. In general, the energy gap (ΔE)of a corrosion inhibitor can be used to evaluate its reactivity. The higher the ΔE, the more stable the inhibitor molecule. The lower the ΔE, the more readily the inhibitor molecule is adsorbed onto the metal surface [43]. ΔE value obtained for trimebutine maleate is low. This molecule is therefore unstable and highly reactive. This reactivity confirms its strong adsorption to the metal surface.Moreover, the inhibitory properties of a molecule depend on its values of overall hardness (η) and overall softness (σ) [43]. A molecule that has a high value of σ and a low value of η is likely to react with the metal to form covalent bonds. Whereas a molecule with a high η value and a low σ value is less reactive. The results indicate that trimebutine maleate has a low η value and a high σ value. This shows that TM is very reactive.

Ionisation energy (I) and electronic affinity (A), which are associated with HOMO and LUMO energies respectively, are descriptors of a molecule's reactivity [44]. These parameters describe the electronic exchanges between the molecule and the metal. The I and A values obtained show that trimebutine maleate has a strong capacity to supply electrons to aluminum.

The electronegativity value (χ) of trimebutine maleate (4.1947 eV) is lower than that of aluminium (4.28 eV), which justifies that the fraction of electrons transferred $\Delta N > 0$. Thus, there is a strong attraction of electrons towards aluminium [7]. This strong attraction that aluminium possesses will contribute to the replacement of its electrons lost during its oxidation in the corrosive medium HCl-2M. These data confirm the experimental values. The electrophilic character of the inhibitor is justified by its high value of the electrophilicity index (ω)[45]. The reaction activity of a molecule also depends on its total energy (E_T). In our work $E_T < 0$, this reflects that there is a charge transfer between the inhibitor and the aluminium [46].

The charge density distribution at each molecular orbital is shown in Figure 13. This charge distribution describes the active regions of the inhibitor. Analysis of Figure 13 indicates that the charge distribution at the HOMO and LUMO orbital is localised towards the nitrogen (N) atom, the carbon C(25) and π-bonds. The charge distribution around the nitrogen and C(25) indicates that these atoms are at the centre of the electronic exchanges allowing the formation of covalent bonds with the empty orbital of the metal. These data confirm the formation of the protective film as indicated by the gravimetric tests.

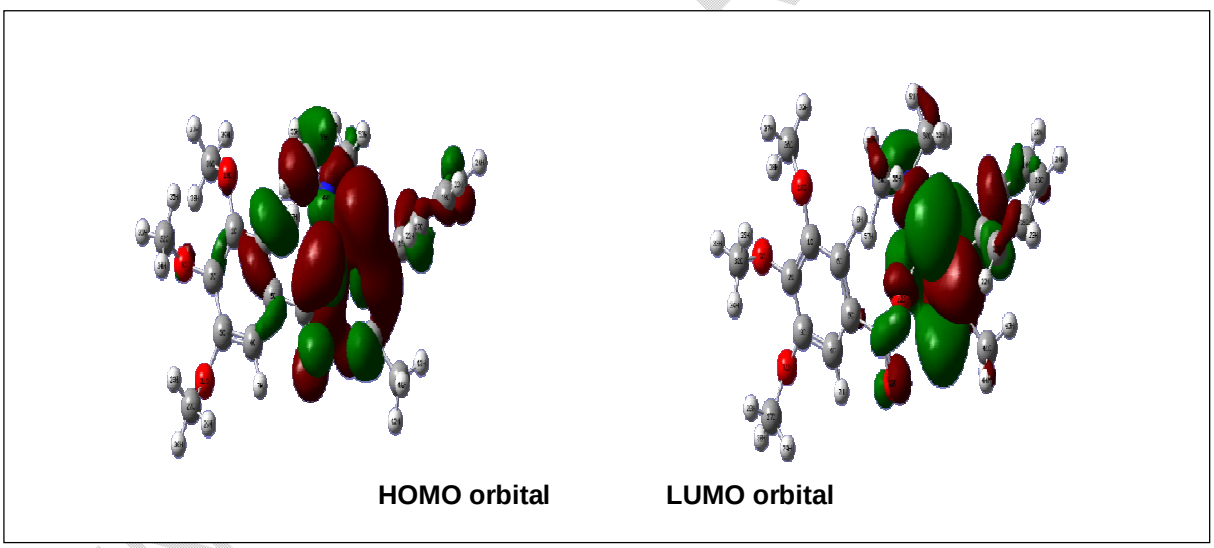

Fig. 13.LUMO and HOMO molecular orbitals density distributions of trmebutine

3.5.2 Analysis of local reactivity parameters

The local reactivity parameters were determined from the Fukui and dual descriptor functions. The values of these parameters are given in Table 6.

Table 6.Mulliken atomic charges, Fukui functions and dual descriptor of trimebutine maleat by B3LYP/6-311G (d, p)

Atoms	$q_k(N+1)$	$q_k(N)$	$q_k(N-1)$	f_k^+	f_k^-	$\Delta f_k(\mathbf{r})$
1 C	0.006593	0.320657	-0.002456	-0.314064	0.323113	-0.637177
2 C	-0.004618	0.252848	0.128018	-0.257466	0.12483	-0.382296
3 C	0.002585	0.316542	-0.040039	-0.313957	0.356581	-0.670538
4 C	-0.00124	-0.135582	0.059392	0.134342	-0.194974	0.329316
5 C	0.000325	0.058641	0.00761	-0.058316	0.051031	-0.109347
6 C	0.002526	-0.13034	0.108356	0.132866	-0.238696	0.371562
7 H	0.000071	0.121994	-0.002936	-0.121923	0.12493	-0.246853
8 H	-0.000261	0.134077	-0.005251	-0.134338	0.139328	-0.273666
9 O	0.005721	-0.504444	-0.01697	0.510165	-0.487474	0.997639
10 O	0.035233	-0.54433	-0.012062	0.579563	-0.532268	1.111831
11 C	-0.001553	0.523937	0.183391	-0.52549	**0.340546**	**-0.866036**
12 O	0.008031	-0.521188	-0.00165	0.529219	-0.519538	1.048757
13 C	0.07198	0.069634	0.197821	0.002346	-0.128187	0.130533
14 C	0.086158	-0.178894	0.001872	0.265052	-0.180766	0.445818
15 C	0.062089	-0.116934	0.003863	0.179023	-0.120797	0.29982
16 C	0.037053	0.076503	-0.001414	-0.03945	0.077917	-0.117367
17 C	-0.025469	-0.151162	0.000827	0.125693	-0.151989	0.277682
18 C	0.086276	-0.112852	0.001309	0.199128	-0.114161	0.313289
19 C	-0.014494	-0.066134	-0.000177	0.05164	-0.065957	0.117597
20 H	-0.003562	0.073477	0.000012	-0.077039	0.073465	-0.150504
21 H	0.018948	0.103269	0.000199	-0.084321	0.10307	-0.187391
22 H	0.00067	0.089262	-0.000142	-0.088592	0.089404	-0.177996
23 H	-0.003151	0.077798	-0.00007	-0.080949	0.077868	-0.158817
24 H	0.001522	0.081005	0.000175	-0.079483	0.08083	-0.160313
25 C	-0.010496	-0.032399	-0.000309	0.021903	-0.03209	0.053993
26 C	0.003525	-0.232111	-0.001941	0.235636	-0.23017	0.465806
27 C	0.000117	-0.125157	-0.000403	0.125274	-0.124754	0.250028
28 H	-0.000039	0.12098	0.000393	-0.121019	0.120587	-0.241606
29 H	-0.000007	0.129352	0.000026	-0.129359	0.129326	-0.258685
30 H	-0.000002	0.137947	-0.000259	-0.137949	0.138206	-0.276155
31 O	-0.000034	-0.521641	0.000602	0.521607	-0.522243	1.04385
32 C	-0.000249	-0.095071	0.008689	0.094822	-0.10376	0.198582
33 H	-0.000026	0.133191	0.001989	-0.133217	0.131202	-0.264419
34 H	0.002857	0.109765	0.001441	-0.106908	0.108324	-0.215232

35	H	-0.000144	0.120314	-0.000791	-0.120458	0.121105	-0.241563
36	**C**	0.538722	-0.376941	0.174696	**0.915663**	-0.551637	**1.4673**
37	H	-0.037707	0.216559	-0.035661	-0.254266	0.25222	-0.506486
38	H	-0.011583	0.200869	0.065469	-0.212452	0.1354	-0.347852
39	H	-0.015435	0.190181	0.043525	-0.205616	0.146656	-0.352272
40	O	0.000572	-0.44954	0.074192	0.450112	-0.523732	0.973844
41	C	-0.000133	-0.320777	0.000308	0.320644	-0.321085	0.641729
42	H	0.000011	0.112275	-0.000003	-0.112264	0.112278	-0.224542
43	H	0.000245	0.113031	-0.00006	-0.112786	0.113091	-0.225877
44	H	-0.000003	0.116251	0.000034	-0.116254	0.116217	-0.232471
45	H	0.000661	0.14474	-0.000024	-0.144079	0.144764	-0.288843
46	H	0.001286	0.124103	0.008373	-0.122817	0.11573	-0.238547
47	H	-0.012284	0.124786	0.022245	-0.13707	0.102541	-0.239611
48	H	-0.005768	0.176185	0.004107	-0.181953	0.172078	-0.354031
49	C	-0.002307	-0.207423	0.002937	0.205116	-0.21036	0.415476
50	H	0.000976	0.095475	-0.000193	-0.094499	0.095668	-0.190167
51	H	0.001284	0.135413	-0.001399	-0.134129	0.136812	-0.270941
52	H	0.010493	0.164515	0.000008	-0.154022	0.164507	-0.318529
53	C	0.122651	-0.172226	0.013794	0.294877	-0.18602	0.480897
54	H	-0.005648	0.150662	0.002915	-0.15631	0.147747	-0.304057
55	H	0.02092	0.129327	-0.000812	-0.108407	0.130139	-0.238546
56	H	0.011181	0.160569	-0.000172	-0.149388	0.160741	-0.310129
57	N	0.014929	-0.410989	0.006606	0.425918	-0.417595	0.843513

The values displayed in Table 6 reveal that C(11) atom has the lowest value of $\Delta f_k(r)$, while the C(36) atom has the highest value of $f_k^+$and $\Delta f_k(r)$. In this context according to Martínez-Araya [47], C(11) and C(36) are respectively the likely sites for electrophilic and nucleophilic attacks. These sites are associated respectively with HOMO and LUMO orbitals of the molecule under study. These results explain the charge distribution around the C(36) atom

4. CONCLUSION

The use of corrosion inhibitors is a means of combating the dissolution of metals. The inhibition efficiency of aluminum corrosion in 2 M HCl by (R,S)-2-(dimethylamino)-2-phenylbutyl 3,4,5-trimethoxybenzoate or trimebutine maleate has been investigated using gravimetric measurement and quantum chemical calculations at DFT/B3LYP/6-31G (d, p) level of theory. The following conclusions were drawn from this study:

- TMacts as a good inhibitor for corrosion of aluminum in 2.0 M HCl solution. The inhibition efficiency increases with increasing concentration.

- The inhibition action is performed via adsorption of the compounds on aluminum surface. The adsorption process is spontaneous and follows Langmuir adsorption isotherm.
- Increasing temperature reduces TM inhibition efficiency, indicating that the adsorption process is dominated by physical adsorption.
- The presence of the extract increases the activation energy of the corrosion reaction.
- Quantum descriptors indicate that trimebutine maleate has a good capacity to accept and donate electrons to the metal.
- The sites of reactivity within the molecule were determined. These sites are mainly carbon atoms.

REFERENCES

1. Jian Z et al. Combining experiment and theory researches to insight into anticorrosion nature of a novel thiazole derivative. *Journal of the Taiwan Institute of Chemical Engineers*, 2021;122: 190-200.

2. Ahmed YM, Abdul AHK, Abu BM, Mohd ST. Experimental and theoretical study on the inhibition performance of triazole compounds for mild steel corrosion.*Corrosion Science*, . 2010;52(10):3331-3340

3. Abdallah M et al. Appraisal of Adsorption and Inhibition Effect of Expired Micardis Drug on Aluminum Corrosion in Hydrochloric Acid Solut. *InternationalJournal of Electrochemical Science,*2022;17(4): 220-462.

4. Nada A, Belal E, Ahmed F, Areej AlB, Arafat T. Investigation of Expired Ticarcillin and Carbenicillin Drugs for Inhibition of Aluminum Corrosion in Hydrochloric Acid Solution. *International Journal of Electrochemical Science*, 2022;17(12): 2212113.

5. Sumayah B, Abhinay T, Hassane LH, Ill-Min C, Kumar A. Corrosion inhibition efficiency of bronopol on aluminium in 0.5 M HCl solution: Insights from experimental and quantum chemical studies. *Surfaces and Interfaces*,2020;20:100-542

6. Khalid HR, Anees AK, Salman HA , Khalida FA-A, Hameed B.M. Optimization studies of expired mouthwash drugs on the corrosion of aluminum 7475 in 1 M hydrochloric acid: Gravimetrical, electrochemical, morphological and theoretical investigations.*Results in Surfaces and Interfaces*, 2023;13:100-165.

7. Bashir Set al. Electrochemical Behavior and Computational Analysis of Phenylephrine for Corrosion Inhibition of Aluminum in Acidic Medium. *Metallurgical and Materials Transactions*,2019;50: 468–479

8. Eddy N.O., Momoh-Yahaya H, Oguzie EE, Theoretical and experimental studies on the corrosion inhibition potentials of some purines for aluminium in 0.1 M HCl. *Journal of Advanced Researc,* 2015;6(2): 203-217.

9. Abdel Hameed RS, Ismail EA, Abu-Nawwas AH, Hussin IA-S, (Expired Voltaren Drugs as Corrosion Inhibitor for Aluminium in Hydrochloric Acid,International. *Journal of Electrochemical Science*,2015;10(3): 2098-2109.

10. Namrata C, Vinod KS, QuraishiMA, Papaya peel extract as potential corrosion inhibitor for Aluminium alloy in 1M HCl: Electrochemical and quantum chemical study,Ain Shams Engineering Journal, 2018; 9(4):1131-1140.

11. Tianqi C, Hui G, Zhan C, Mengjin C, Chaoyang Fu,Eco-friendly approach to corrosion inhibition of AA5083 aluminum alloy in HCl solution by the expired Vitamin B1 drugs. *Journal of Molecular Structure*, 2021; 1244: 130-881

12. Zhang W, Buchheit RG, Effect of ambient aging on inhibition of oxygen reduction by chromate conversion coatings. *Corrosion,*2003;59(4):356-362.

13. Abdelkader K, Abdellah K, Kamel H, Razika M, Thymus algeriensis extract as a new eco-friendly corrosion inhibitor for 2024 aluminium alloy in 1M HCl medium. *Journal of Molecular Liquids*, 2016;214(201): 293-297.

14. Desai PS, Falguni D, Adarsh P, Bhumika P, Anticorrosive properties of Eucalyptus (Nilgiris) leaves extract on 2S grade aluminium in acid solutions. *Applied Surface Science Advances*, 2023;16: 400-41.

15. Radouane et al. Experimental assessment and molecular-level exploration of the mechanism of action of Nettle (Urtica dioica L.) plant extract as an eco-friendly corrosion inhibitor for X38 mild steel in sulfuric acidic medium, Arabian Journal of Chemistry, 2023;16 (8): 104-988

16. Ebenso EE, Arslan T, Kandemirli FNC, Love I, Quantum chemical studies of some rhodanine azosulpha drugs as corrosion inhibitors for mild steel in acidic medium. *International Journal of Quantum Chemical*,2010; 110: 1003-1018.

17. Abdallah M, Zaafarany I, Al-Karanee SO, Abd El-Fattah AA,). Antihypertensive drugs as an inhibitor for corrosion of aluminum and aluminum silicon alloys in aqueous solutions, *Arabian Journal of Chemistry*, 2012;5: 225-234.

18. 18.Amadou K, et al. Copper Corrosion Inhibition in 1M HNO3 by Loratadine: A Combined Experimental and Theoretical Study. *International Journal of Materials and Chemistry*, 202010(3): 31-43

19. Tigori MA, Kouyaté A, Assouma DAC, Kouakou V, Niamien PM, Theoretical Investigation of Two Antidiabetics Drugs as Corrosion Inhibitors of Aluminium in 1.0 M HCl: Combining DFT and QSPR Calculations. *American Journal of Materials Science and Engineering*, 2020; 8(1): 6-16

20. Yeo M, Tigori MA, Amadou KA, Niamien PM, Trokourey A, Inhibition of Aluminium Corrosion in 1M HCl by Pyridoxine Hydrochloride: Thermodynamic and Quantum Chemical Studies. *International Research Journal of Pure & Applied Chemistry*,2020;15:19

21. CisséM, TigoriMA, AssomanKA, KouyatéA, NiamienPM, Gravimetric and Quantum Chemical Approach of Nifuroxazid as Inhibitor of Aluminium Corrosion in 2.0 M HCl. *Journal of Materials Physics and Chemistry,*2024;12(1):1-10

22. Frisch M et al.Gaussian 09.Gaussian, Inc., Wallingford CT,2009..

23. Lee C, Yang W, Parr RG, Development of the Colle-Salvetti correlation-energy formula into a functional of the electron density. *Physical Review B*,1988; 37, 785.

24. Kumara D, Jain N, Rai B, Amino acids as copper corrosion inhibitors: A density functional theory approach.*Applied Surface Science*, 2020;514: 145-905

25. Yang B, Yizhen L, Zhang Z, Xinying H, Zhu Y, Anticorrosion mechanism of natural acidic amino acids on steel in chloride solution: Experimental, theoretical and machine learning approaches. *Journal of Building Engineering* , 2023; 79: 107-801

26. 26. ParrRG, Pearson RG, Absolute hardness:companion parameter to absolute electronegativity. Journal of the American chemical society, 1983;105(26), 7512-7516

27. Chirico N, Gramatica P, Real external predictivity of QSAR models. Part 2. New intercomparable thresholds for different validation criteria and the need for scatter plot inspection. Journal of chemical information and modeling, 2012; 52(8), 2044-2058

28. Pearson RG, Absolute electronegativity and hardness correlated with molecular orbital theory. Proceedings of the National Academy of Sciences, 1986; 83(22), 8440-8441

29. Parr RG, Szentpály LV, Liu S, Electrophilicity index. Journal of the American Chemical Society, 1999;121(9), 1922-1924

30. Cissé M, Tigori MA, Assoman KA, Kouyaté A, Niamien PM,Gravimetric and Quantum Chemical Approach of Nifuroxazid as Inhibitor of Aluminium Corrosion In 2.0 M HCl. *Journal of Materials Physics and Chemistry*, 2024;12(1):1-10.

31. LangmuirI, The constitution and fundamental properties of solids and liquids, Journal of the American Chemical Society, 1916; 38(11):2221–2295.

32. Temkin MI, Adsorption equilibrium and process Kinetics on inhomogeneous surfaces with interaction between adsorbed molecules. Zh. Fiz. Khim, 1941; 15(3):296-332.

33. Freundlich H, Uber die adsorption in losungen, Z Physical Chemistry, 1906; 57:385–470.

34. Awady YAE, Ahmed AI, Effect of temperature and inhibitors on the corrosion of aluminium in 2N HCl solution, A kinetic study. Journal of Indian Chemistry,1985; 24 :601-606.

35. Adejo SO, Proposing a new empirical adsorption isotherm known as Adejo-Ekwenchi isotherm. *J. Appl. Chem*, 2014; *6*(5), 66-71.

36. Adejo SO, Ahile JU, Gbertyo JA, Kaior A, Ekwenchi MM, Resolution of adsorption characterisation ambiguity through the Adejo-Ekwenchi adsorption isotherm: a case study of leaf extract of Hyptis suaveolen poit as green corrosion inhibitor of corrosion of mild steel in 2 M HCl. *Journal of Emerging Trends in Engineering and Applied Sciences*, 2014; 5(8): 201-205.

37. Abdallah M et al. Natural nutmeg oil as a green corrosion inhibitor for carbon steel in 1.0 M HCl solution: Chemical, electrochemical, and computational methods. *Journal of Molecular Liquids*, 2021; 323: 115036.

38. Toghan A, Gadow HS, Dardeer HM, Elabbasy HM, New promising halo- genated cyclic imides derivatives as potential corrosion inhibitors for carbon steel in hydrochloric acid solution. *Journal of Molecular Liquids*, 2021;325: 115-136.

39. Allah MD, El Hefnawy M, Elhamed SA, Experimental investigation of the corrosion inhibition of Aluminum by three novel anionic surfactants as green inhibitors in HCl solution. *Chemical Data Collections*, 2023;45: 101033.

40. Singh AK, Mohapatra S, Pani B, Corrosion inhibition effect of Aloe Vera gel: Gravimetric and electrochemical study. *Journal of Industrial and Engineering Chemistry,*2016;33: 288-297.

41. Zeng J,Gan Y,Xu Z,Zhu H, Tan B,Li W, Adsorption films based on indazole derivatives for application to protect Cu in sulfuric acid: Experimental and theoretical approaches. Journal of the Taiwan Institute of Chemical Engineers, 2023;151: 105-134.

42. Issaadi S, Douadi T, Chafaa S,Adsorption and inhibitive properties of a new heterocyclic furan Schiff base on corrosion of copper in HCl 1M: Experimental and theoretical investigation.*Applied Surface Science*, 2014; 316: 582-589.

43. Ebaz AO, Karzan MA, Shalaw KS, Karzan AO, Wali MH, Dyari MM, N,N-Bis (2,4-dihydroxy benzaldehyde) benzidine: Synthesis, characterization, DFT, and theoretical corrosion study.*Journal of Molecular Structure*, 2024;1300: 137-279.

44. Zhang SG, Lei W, Xia MZ & Wang FY, QSAR Study on N-Containing Corrosion Inhibitors: Quantum Chemical Approach Assisted by Topological Index. *Journal of Molecular Structure*: THEOCHEM, 2005; 732:173-182.

45. AhmedA, Corrosion inhibition effect of 2-N-phenylamino-5-(3-phenyl-3-oxo-1-propyl)-1,3,4-oxadiazole on mild steel in 1 M hydrochloric acid medium: Insight from gravimetric and DFT investigations, Materials Science for Energy Technologies, 2021; 4 :398-406

46. Tigori MA, KouyatéA, KouakouV, Niamien PM, TrokoureyA, Computational approach for predicting the adsorption properties and inhibition of some antiretroviral drugs on copper corrosion in HNO3. European Journal of Chemistry, 2020;11 (3):235-244

47. Martínez-Araya JI, Why is the dual descriptor a more accurate local reactivity descriptor than Fukui functions? The Journal of Mathematical Chemistry, 53, 451–465(2015)